

Iterative Deformable FEM Model for Nonrigid PET/MRI Breast Image Coregistration

Mehmet Z. Unlu¹, Andrzej Krol^{2,1,3}, Alphonso Magri³, David H. Feiglin², James A. Mandel⁴,
Edward D. Lipson^{3,1,2}, Ioana L. Coman^{5,1,2}, Wei Lee¹, and Gwen Tillapaugh-Fay²

¹Department of Electrical Engineering and Computer Science, Syracuse University

²Department of Radiology, SUNY Upstate Medical University

³Department of Physics, Syracuse University

⁵Department of Mathematics and Computer Science, Ithaca College

⁴Department of Civil and Environmental Engineering, Syracuse University

ABSTRACT

We implemented an iterative nonrigid registration algorithm to accurately combine functional (PET) and anatomical (MRI) images in 3D. Our method relies on a Finite Element Method (FEM) and a set of fiducial skin markers (FSM) placed on breast surface. The method is applicable if the stress conditions in the imaged breast are virtually the same in PET and MRI. In the first phase, the displacement vectors of the corresponding FSM observed in MRI and PET are determined, then FEM is used to distribute FSM displacements linearly over the entire breast volume. Our FEM model relies on the analogy between each of the orthogonal components of displacement field, and the temperature distribution field in a steady state heat transfer (SSHT) in solids. The problem can thus be solved via standard heat-conduction FEM software, with arbitrary conductivity of surface elements set much higher than that of volume elements. After determining the displacements at all mesh nodes, moving (MRI) breast volume is registered to target (PET) breast volume using an image-warping algorithm. In the second iteration, to correct for any residual surface and volume misregistration, a refinement process is applied to the moving image, which was already grossly aligned with the target image in 3D using FSM. To perform this process we determine a number of corresponding points on each moving and target image surfaces using a nearest-point approach. Then, after estimating the displacement vectors between the corresponding points on the surfaces we apply our SSHT model again. We tested our model on twelve patients with suspicious breast lesions. By using lesions visible in both PET and MRI, we established that the target registration error is below two PET voxels. The surface registration error is comparable to the spatial resolution of PET.

Key words: nonrigid image registration, finite element method, deformable model, multimodal, MRI/PET breast image registration, warping, fiducial skin markers

1. INTRODUCTION

Medical imaging modalities such as CT, MRI, and PET provide highly specialized information depending on their scanning methods. Therefore, thorough information about the volumes of interest such as tumors, organs, and anatomy cannot be provided using information solely from one modality. Registering two image volumes and then creating a composite image provides complementary information that can be viewed simultaneously, so that direct comparisons and assessments can be made [1]. Image-processing techniques and algorithms are needed to compute geometrical differences between 3D scans of a given region of interest in different modalities, or in the same modality at different times, and to register the respective scans. Nonrigid registration of multimodality images is in an early stage of development. A number of commercial devices such as PET/CT and SPECT/CT are available for this purpose and they are very useful for registering and fusing images obtained almost simultaneously from two different modalities. However, for practical and economical reasons, MRI and PET scanners cannot be combined into one device. For that reason, appropriate imaging protocols and image processing methods are needed to register and fuse MR and PET images.

In the context of PET/MRI multimodal breast imaging, a nonrigid approach is necessary, and here we present a new image acquisition and processing protocol, and a methodology that relies on a finite element method (FEM) deformable

breast model and on the use of a set of fiducial skin markers (FSMs) placed on the breast surface for nonrigid 3D breast image co-registration. This approach does not require any information on patient-specific breast morphology and elastic tissue properties. However, it can be applied only if the stress conditions in the imaged breast are virtually the same between moving and target images. This is accomplished by use of identical patient support and positioning systems in both modalities.

The registration model consists of two steps. In the first step, the displacements between the corresponding FSMs observed in moving and target images are determined and FEM is used to distribute the FSM displacements linearly, first over the breast surface and then over the entire breast volume. Our FEM model relies on the analogy between each orthogonal component of the displacement field and the temperature field in a steady state heat transfer (SSHT) in solids. This analogy is valid because the displacement field in the x , y , and z directions and a the temperature field in SSHT can both be modeled using Laplace's equation, and the displacements can be considered to be analogous to the temperature differences in SSHT. Such an FEM problem can be solved via standard heat conduction FEM software with the arbitrary conductivity of surface elements set much higher than that of volume elements. After determining, by this analogy, the displacements at all the mesh nodes, the moving breast volume is registered to the target breast volume using an image-warping algorithm. In the second step, to correct for any residual surface and volume misregistration, displacements are estimated for a large number of corresponding points on already grossly aligned MRI and PET breast surfaces, and the SSHT FEM model is applied again. In this paper we evaluate the performance of our nonrigid registration method in the context of combined PET and MRI breast cancer imaging.

2. MATERIALS AND METHODS

We have developed and implemented an imaging strategy and a suitable FEM model along with a surface refinement process for nonrigid registration of intra- and intermodal medical breast images. This approach does not require any information on patient-specific breast morphology and elastic tissue properties. However, it can be applied only if the stress conditions in the imaged breast are virtually the same between moving and target images. This is accomplished by the use of identical patient support and positioning systems in both modalities. Under these conditions, the observed intra- and intermodality displacements, after rigid alignment of moving and target images, are predominantly due to underlying biological and physical differences in the imaging process and in the reconstruction algorithm used, including differences in the scanners' spatial distortions and resolution, and signal-to-noise ratio [2,3]. Our model compensates for these dissimilarities. In addition, it compensates for small discrepancies in patient positioning and for minor displacements resulting from physiological and other motion. The model can be classified as a point-based registration method combined with a deformable finite element method breast model and requires a small number of non-invasive fiducial skin markers (FSMs) visible in PET and MRI placed on the surface of the examined breast. Below, we present the methodology including a) data acquisition; b) preprocessing and rigid registration; c) fiducial-skin-marker localization; d) surface extraction and 3D FEM model creation; e) model deformation; f) warping algorithm and interpolation of FEM results; and g) surface refinement using a surface-matching algorithm. Figure 1 shows the general block diagram of the algorithm presented.

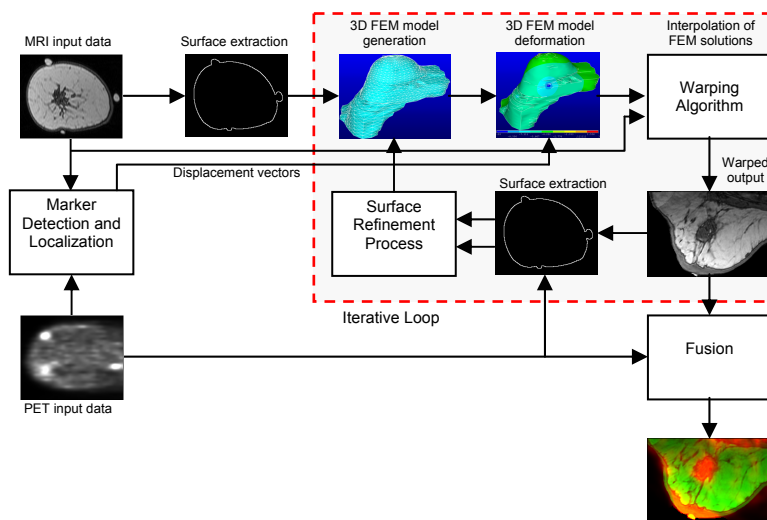


Fig. 1. General block diagram of the method.

2.1. Data acquisition

The data were acquired using a dedicated PET/CT scanner (GE Discovery ST with BGO detector and 4-slice CT) and a 1.5 T MRI system (Philips Intera). PET images were obtained with patient prone and the breasts freely suspended immediately after intravenous administration of 10 mCi of F-18-FDG with nine fiducial skin markers (FSM) taped on each breast. They were reconstructed in $128 \times 128 \times 47$ matrix with 4.25 mm voxel size. Each FSM contained about 0.5 μCi of Ge-68. In MRI scans, the patient was prone with both breasts suspended into a single well housing the standard Philips clinical breast RF receiver coil. A high-resolution 3D Fast Field Echo (FFE) technique, with $\text{TR/TE} = 14/3$, was applied to obtain MRI breast images. An image matrix of $512 \times 512 \times 120$ was used in reconstruction with $0.7 \times 0.7 \times 1.4 \text{ mm}^3$ voxel size. The field of view ($360 \text{ mm} \times 360 \text{ mm}$) was centered over the breasts.

2.2. Preprocessing and rigid registration

Before carrying out the general steps of our algorithm, the MRI and PET data need to be preprocessed and rigidly registered. To preprocess the data, the steps listed below are applied. The preprocessing scheme was performed automatically by using our own custom plug-ins in the ImageJ¹ software environment. Individual steps was applied to the data as needed.

- Open PET, CT and MRI images in axial view.
- Normalize PET data to bring all the slices into same level of contrast.
- Bring all images into same orientation. Usually, it is carried out according to MRI data. The resulting images are in prone position, and the slices are arranged from posterior to anterior.
- Convert PET, CT, and MRI data to isotropic matrix of the smallest voxel size on the dimensions available which is usually the voxel size of MRI data in x and y direction of axial view.
- Crop the images in 3D while performing rigid registration.
 - PET and CT images, need to have their sizes the same as MRI
 - Rigid registration process is performed using coordinates of centroids of two markers placed on the left and on the right side of the patient. To achieve that, first a 3D cropping window in PET image space with the same size as MRI image is created. Then the window is shifted appropriately until the distance between the markers and the vertices of the cropping window in 3D is the same as the distance between the marker centroids and the vertices of MRI image in 3D. As a result, the corresponding markers located on the patient's left and right sides, as well as the images of the patient in PET/CT and MRI, are rigidly registered.

¹ <http://rsb.info.nih.gov/ij/>

2.3. Fiducial skin markers and displacement vectors

Fiducial skin markers (FSMs) used for MRI scans are placed in the same locations as the FSMs used in PET studies to sample the displacement between the moving and the target images (Fig. 2). The locations of FSMs are marked in ink on the patient's skin to ensure that both types of marker are placed in the same locations. The corresponding pairs of markers are manually defined in the target (PET) and in the moving (MRI) images. The localization of markers is performed by calculating the intensity-based centroids, using the method described by Wang *et al.* [4]. In this iterative knowledge-based method, a user first identifies a voxel belonging to a marker, and then the algorithm finds the lowest threshold, which defines a set of voxels connected in 3D to a selected voxel, thus forming an object with proper geometrical extent in 3D to be a marker. The effective size of the marker is defined by the spatial resolution of the system. Since our registration method uses only a small number of FSMs and this might result in misregistration in some breast regions away from FSMs, we implemented an iterative approach to nonrigid image registration.

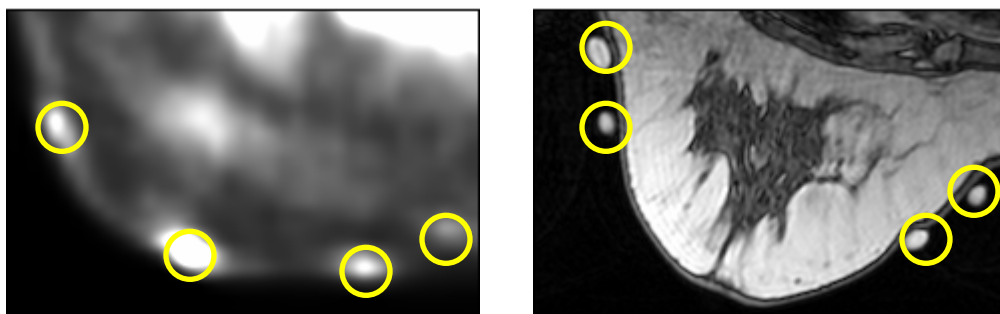


Fig. 2. Example of fiducial skin markers on same breast surface in PET (left panel) and MR (right panel) images

2.4. Patient-specific surface-geometry construction

Patient specific geometry of the breast is obtained from sagittal or coronal cross sections of the moving image (MRI). It is accomplished by application of a simple thresholding, followed by appropriate image erosion and dilation. As a result, the breast surface contours are outlined in MRI (Fig. 3). The set of breast contours are then used to create an input file for commercial finite element method (FEM) software (ANSYS)². The file contains the geometry of the breast built by key points, splines, and volumes, as well as the definition of the surface and volume elements and the displacement vectors.

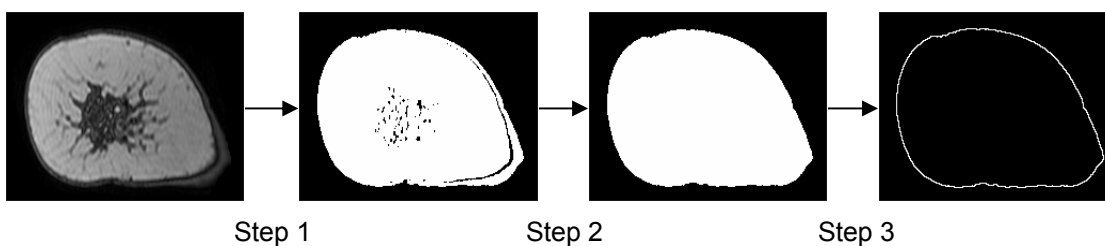


Fig. 3. Consecutive processing steps (left to right) leading to estimation of surface geometry of moving breast image in coronal view.

2.5. 3D FEM model generation and deformation

Our custom written plug-in in ImageJ takes the set of coronal breast contours as an input, and generates the 3D finite element model (FEM) file of the breast to be used as an input by the FEM software (ANSYS)². The file contains the geometry of the breast defined by key points, splines, and volumes, as well as the definition of the surface and volume

² ANSYS ver. 5.7.1 - ANSYS, Inc. Canonsburg, Pennsylvania

elements, and the displacement vectors. The breast surface and volume are meshed by a set of finite elements connected through nodes located on element boundaries (Fig. 4). In this study, triangular surface elements and tetrahedral volume elements are used (Fig. 5). A dense displacement field is then obtained using FEM, by first distributing linearly the Cartesian components of the fiducial displacement vectors over the breast surface and then throughout its volume. Our FEM model uses an analogy between each orthogonal component of the dense displacement field and the temperature distribution in a steady-state heat-transfer (SSHT) problem. After estimation of the displacement vectors at all nodes, the MRI breast mesh is deformed.

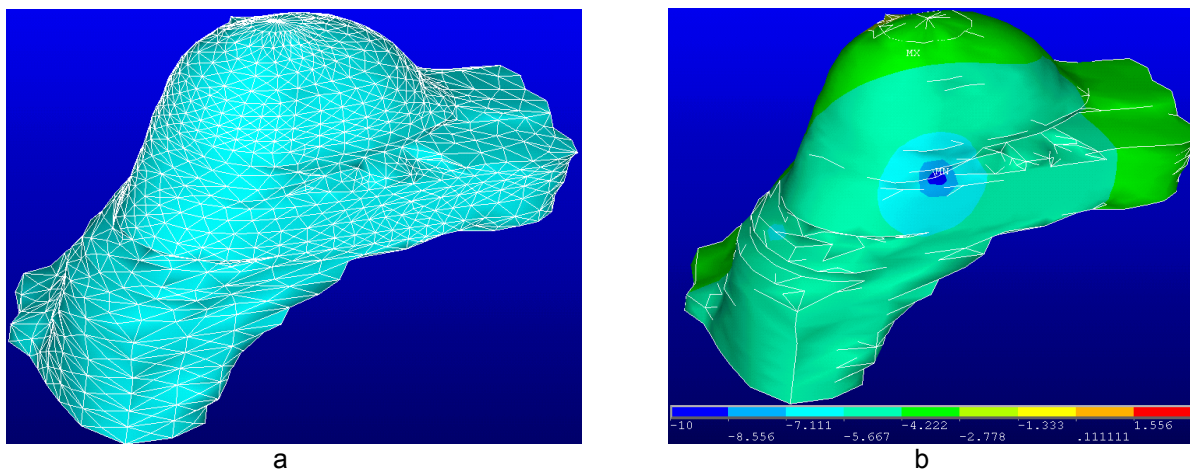


Fig. 4. a. Meshed breast surface and breast volume using ANSYS² package. **b.** Distribution of the marker displacements over the entire breast surface and volume.

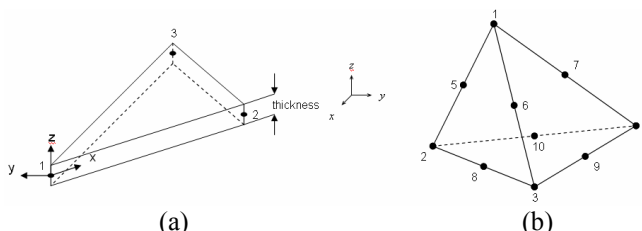


Fig. 5. a. 2-D Thermal Shell mesh element (ANSYS element number: SHELL57) **b.** 3-D 10-Node Tetrahedral Thermal Solid mesh element (ANSYS element number: SOLID70).

2.6. Interpolation of FEM solutions – warping algorithm

The SSHT FEM computation yields a displacement vector at each node of the finite element mesh. Displacement vectors for each location (voxel or subvoxel) within a finite element can be interpolated using a weighted sum of the element's nodal displacements with the weights equal to the element's node shape function [5],

$$\vec{u} = \sum_{i=1}^{N_{nodes}} N_i^{el} \vec{u}_i^{el} \quad (2.1)$$

where N_{nodes} is the number of nodes in the element, N_i^{el} is the element's node shape function, and u_i^{el} is the nodal displacement vector. In this study, the exact FEM interpolation given by Eq. 2.1 is used to obtain the dense displacement field within each FEM element, which in turn is used to interpolate the image gray values via a truncated sinc interpolation kernel. This process is called warping of the moving (floating) image to the target (fixed) image. We emphasize that only the voxels inside the FEM mesh are affected by this kind of processing.

2.7. Second iteration: Refinement process

After obtaining the warped image of MRI, a surface-matching algorithm is applied to correct small surface and volume discrepancies. In this step, instead of using fiducial marker displacements, which have already been aligned, we use the displacements of selected corresponding surface points, to determine the transformation between the two images. For this purpose, surface regions that need to be refined are first determined and represented by the curves in 2D using cubic-spline representations of the moving and the target images. Then, using the closest-distance criterion, the corresponding points on the target-image surface are determined for each of the selected points on the moving image. Using the distances between the corresponding points in the moving and in the target images, via application of our FEM model, the moving image is deformed for a second time. Further, using the same analogy and the method described in Sec. 2.5, the displacements are distributed over the entire mesh volume and the target and the moving images are registered using the warping algorithm. Finally, nonrigidly registered moving (MRI) and target (PET) images are fused.

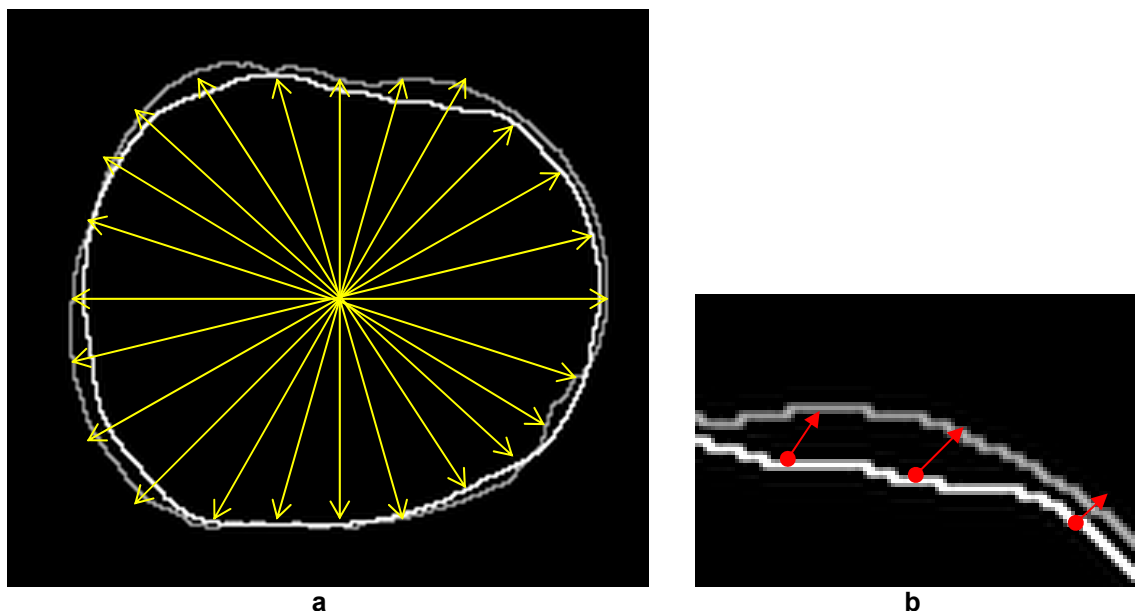


Fig. 6. a. Definition of corresponding points on the surfaces of the moving and the target images. Gray: CT (PET) surface, White: MRI surface. b. Partial zoomed view of displacement vectors obtained for previously defined (left panel) corresponding points on the surfaces.

3. EXPERIMENTAL STUDIES

We have acquired PET and MRI data with fiducial skin markers on a number of patients, using the protocols and the processing methodology described in Sec. 2. We have applied our SSHT FEM registration technique to perform multimodal PET-MRI registration in 3D. To assure that the stress conditions in the imaged breast are virtually the same in different modalities, we used the replica of the MRI breast antenna made of plastic with very low absorption for 511 keV photons in PET scans. The high-resolution MRI scan, currently obtained for anatomical purposes, works very well for defining the surface of the breast. This 3D T1-weighted sequence has been applied without fat saturation, so that the skin surface is easily visualized. The signal arising from skin is 16 times above the noisy background observed in the vicinity of the breast. Voxels are obtained with nearly isotropic resolution and with an edge dimension of 1.2 mm. These factors permit automated computer segmentation via simple thresholding with good definition of the breast surface to be used to create an FEM mesh with the ANSYS package. The geometric centroids of fiducial markers visible in PET and MRI were estimated using the iterative knowledge-based method described in Sec. 2.3, and the discrete displacement field was obtained. These data allowed our FEM model to obtain a dense displacement field (*i.e.* a displacement vector for each mesh node), which in turn was used to warp in 3D the moving MRI image to the target

PET image. Registered images were fused using the KGB Fusion Viewer³ program. In the following examples coregistered images have been fused using a frame-by-frame approach; a “fire” pseudocolor scheme has been used to display low resolution functional F-18-FDG PET data, and gray scale was used to display high-resolution anatomical MRI data. After applying these color schemes, the resulting images were averaged with equal weight.

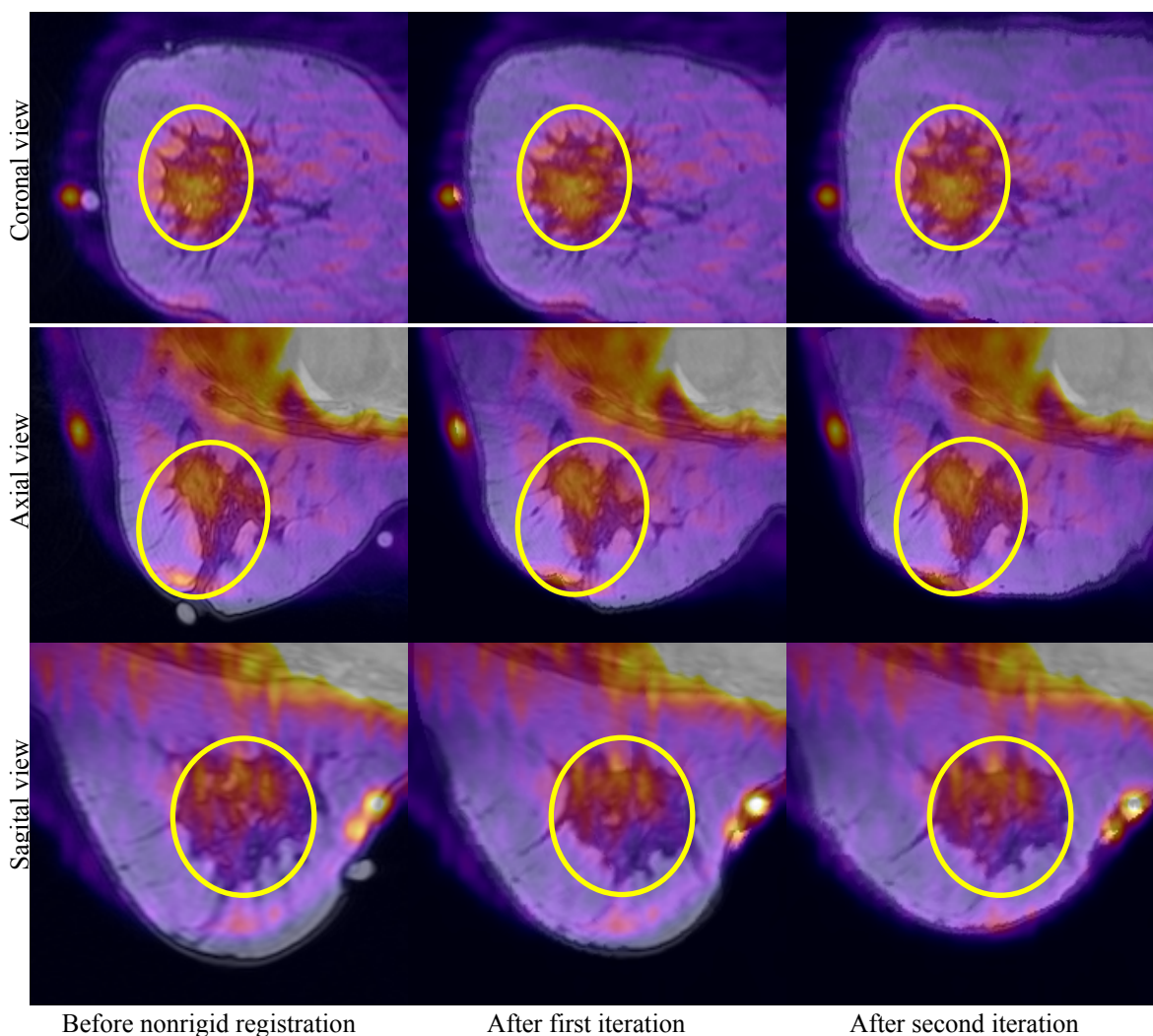


Fig. 7. Comparison of coregistered functional (PET) and anatomical (MRI) breast images. Fire pseudocolors: PET. Gray scale: MRI (subject 28 – right breast).

4. EVALUATION OF REGISTRATION RESULTS

We evaluated performance of our method using both qualitative and quantitative measures on PET and MRI breast images obtained for a small number of patients with difficult-to-read or equivocal mammograms or ultrasound breast exams. These patients were imaged with PET and MRI, as described above. Our iterative FEM deformable model for nonrigid registration of PET-MRI breast images yielded good results, allowing accurate nonrigid registration of functional and anatomical data (Fig. 7). To evaluate the results, we applied three different qualitative similarity estimates: a) isoprojected surface similarity (ISS); b) normalized polar-plot surface similarity (NPSS); and c) z -axis surface similarity (ZSS). The ISS graph is a surface projection image in which the intensity values represent distances between the corresponding points on two surfaces (Fig. 8). The ISS graph allows one to determine where the two

³ <http://www.kgbtechnologies.com/fusionviewer/>

surfaces are well aligned and where they are misaligned. The NPSS plot is similar to the ISS plot, except that it is a polar projection of the surfaces and its center corresponds to the apex layer of the imaged breast (Fig. 9). NPSS has the advantage of allowing comparison of registration results obtained for different patients. The ZSS graph depicts the average difference between corresponding points on the target and the moving images vs. cross-section location along arbitrary z-axis (Fig. 10). We also performed error analysis to investigate how our method behaves when the number of FSMs is changed (Fig. 11a) and to determine the relationship between target-registration and the fiducial-marker-localization errors (Fig. 11b). We performed error studies using 23 selected region-of-interest (ROIs) inside a breast.

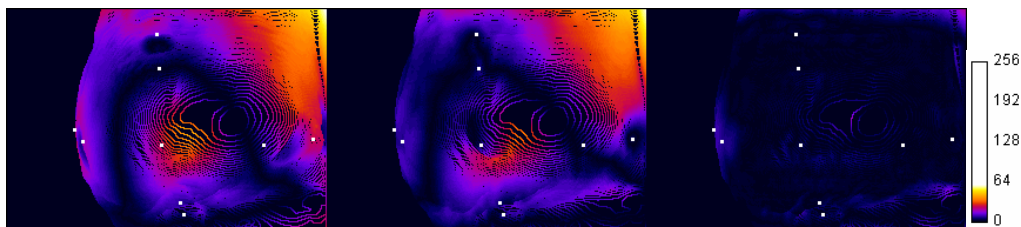


Fig. 8. ISS – Isoprojected surface-similarity plot for subject 28, used for comparison of surface differences between target and moving image of same subject (see text). Dots indicate locations of fiducial markers.

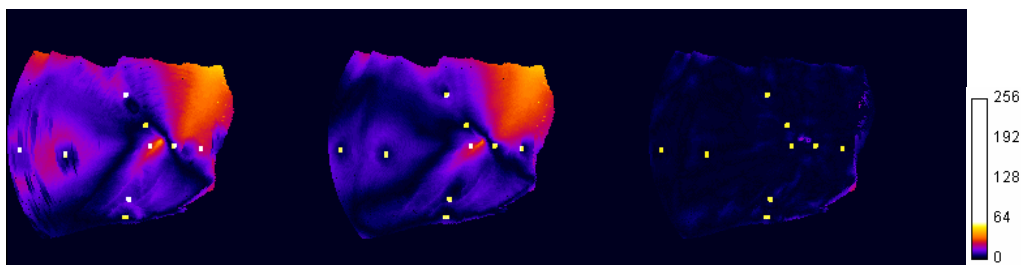


Fig. 9. NPSS – Normalized polar-surface similarity plot for subject 28, used for comparison of surface differences between target and moving image between different subjects (see text). Dots indicate locations of fiducial markers.

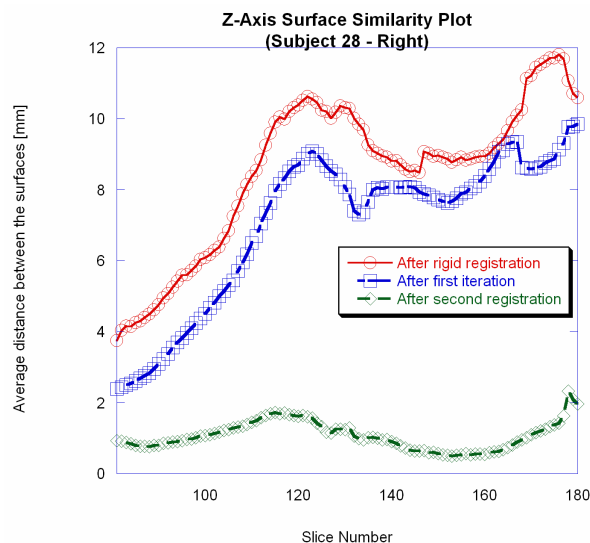


Fig. 10. Z-axis surface similarity plot to compare average and/or maximum surface differences for each corresponding slice.

Table 4.1 Average target registration error (in mm) vs. number of fiducial skin markers (subject 28) for ROIs inside and outside a polyhedron defined by fiducial skin markers.

Number of markers used	After first iteration		After second iteration	
	ROIs outside	ROIs inside	ROIs outside	ROIs inside
9	3.22	0.78	2.13	0.42
7	3.59	0.91	2.56	0.52
5	3.64	1.02	2.48	0.70
4	3.55	1.41	2.61	1.05
3	3.75	1.37	2.93	1.13

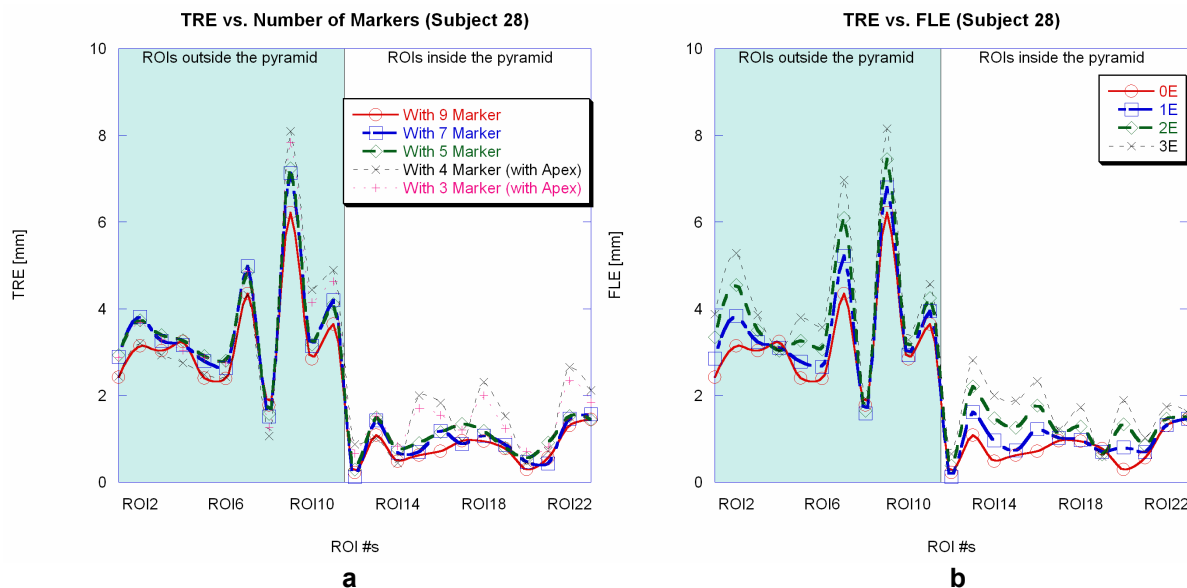


Fig. 11. a. Target registration error vs. number of fiducial skin markers for selected ROIs. **b.** Target registration error vs. fiducial localization error ($\epsilon = 1.7\text{mm}$) for selected ROIs. Shaded region indicate ROIs outside a polyhedron defined by fiducial skin markers.

5. CONCLUSIONS

We have developed a deformable breast model for nonrigid registration of intermodal (PET/MRI) breast images. This model requires fiducial skin markers (FSMs) placed on the breast surface. It also requires careful patient prone positioning to make sure that stress conditions are unchanged between scans. Using our custom software, the geometry of the model is constructed from the moving image via thresholding the breast image and extracting the surface contours, thus allowing the 3D mesh of the model to be obtained using a commercial FEM package (ANSYS). The deformation step starts from initial and boundary conditions determined by FSM displacement vectors. After application of the deformation process, the final deformed model of the breast is obtained and the moving image is registered to the target image. We also applied a refinement process to correct for any residual surface misregistration: the displacements are estimated for a large number of corresponding surface points on the moving and the target breast images, already grossly aligned in 3D, and our model and the warping algorithm are applied for a second time. To present and quantify the results, we implemented three qualitative image-registration estimates called isoprojected surface similarity (ISS), normalized polar-plot surface similarity (NPSS), and z -axis surface similarity (ZSS). We also implemented two different error analyses: target registration error vs. number of fiducial skin markers, and target registration error vs. fiducial localization error. By using the region of interest visible in MRI, we established that the target registration error is below two PET voxels. The surface registration error is comparable to the spatial resolution of PET. The results

showed that the model corrects most of the motion and other image artifacts between the scans and thus allowing for accurate coregistration of functional (PET) and anatomical (MRI) breast images.

6. REFERENCES

- [1] Chen, G.T.Y., C.A. Pelizzari, and D.N. Levin, *Image Correlation in Oncology. Important Advances in Oncology.*, ed. D. Vitav and H. Rosenbergs. 1990, Philadelphia: J.B. Lippincott Co. 131-141.
- [2] Jizzard, P., *Physical Basis of Spatial Distortion in MRI*, in *Handbook of Medical Imaging*, I.N. Bankman, Editor. 2000, Academic Press.
- [3] Dahlbom, M. and S.C. Huang, *Physical and Biological Bases of Spatial Distortion In PET Images*, in *Handbook of Medical Imaging*, I.N. Bankman, Editor. 2000, Academic Press.
- [4] Wang, M.Y., et al., *An automatic technique for finding and localizing externally attached markers in CT and MR volume images of the head*. Biomedical Engineering, IEEE Transactions on, 1996. **43**(6): p. 627 -637.
- [5] Zienkiewicz, O.C. and R.L. Taylor, *The Finite Element Method*. 1987, New York: McGraw Hill Book Co.